

# Locally Subspace-Informed Neural Operators for Efficient Multiscale PDE Solving

**Alexander Rudikov**  
AIRI  
Moscow, Russia  
Rudikov@airi.net

**Vladimir Fanaskov**  
AIRI, Skoltech  
Moscow, Russia

**Sergei Stepanov**  
Institute of Mathematics and Computer Science,  
North-Eastern Federal University  
Yakutsk, Russia

**Buzheng Shan**  
Department of Mathematics  
Texas A&M University  
College Station, Texas, USA

**Ekaterina Muravleva**  
Sberbank, AI4S Center, Skoltech  
Moscow, Russia

**Yalchin Efendiev**  
Department of Mathematics,  
Texas A&M University,  
College Station, Texas, USA

**Ivan Oseledets**  
AIRI, Skoltech  
Moscow, Russia

## Abstract

Neural operators (NOs) struggle with high-contrast multiscale partial differential equations (PDEs), where fine-scale heterogeneities cause large errors. To address this, we use the Generalized Multiscale Finite Element Method (GMsFEM) that constructs localized spectral basis functions on coarse grids. This approach efficiently captures dominant multiscale features while solving heterogeneous PDEs accurately at reduced computational cost. However, computing these basis functions is computationally expensive. This gap motivates our core idea: to use a NO to learn the subspace itself—rather than individual basis functions—by employing a subspace-informed loss. On standard multiscale benchmarks—namely a linear elliptic diffusion problem and the nonlinear, steady-state Richards equation—our hybrid method cuts solution error by approximately 60% compared with standalone NOs and reduces basis-construction time by about 60 times relative to classical GMsFEM, while remaining independent of forcing terms and boundary conditions. The result fuses multiscale finite-element robustness with NO speed, yielding a practical solver for heterogeneous PDEs.

## 1 Introduction

Recent advances in machine learning have sparked growing interest in developing data-driven solvers for partial differential equations (PDEs) Azizzadenesheli et al. [2024], Karniadakis et al. [2021], Kovachki et al. [2023]. This trend led to significant advances in neural operators (NOs), which approximate PDE-to-solution mappings directly from data. Methods like Fourier Neural Operators (FNOs) Li et al. [2020], Kovachki et al. [2023], Factorized FNOs (FFNOs) Tran et al. [2021], and DeepONets Lu et al. [2019] have demonstrated remarkable success in accelerating simulations for problems with smooth or moderately heterogeneous coefficients. However, a critical challenge remains in solving high-contrast, multiscale PDEs—common in real-world applications such as reservoir modeling, composite materials, and subsurface flow—where fine-scale heterogeneities induce large errors in NO predictions. Traditional NOs struggle to capture these localized features

efficiently, often requiring prohibitively large networks or extensive training data to achieve acceptable accuracy.

A well-established numerical approach for such problems is the Generalized Multiscale Finite Element Method (GMsFEM) Efendiev et al. [2011, 2013], Chung et al. [2016], which constructs localized spectral basis functions on coarse grids to resolve multiscale PDEs. By decomposing the problem into local eigenproblems, GMsFEM extracts basis functions that encode fine-scale information, enabling accurate coarse-grid solutions at lower computational cost. However, this accuracy comes at a price: solving these local eigenproblems is computationally expensive.

In recent work Spiridonov et al. [2025], the authors employed a fully connected neural network to predict an additional basis function for the steady-state Richards equation Richards [1931], Farthing and Ogden [2017], supplementing an existing set of precomputed basis functions. While this approach enhanced prediction accuracy, it failed to deliver computational efficiency gains because traditional methods still generated most basis functions. Furthermore, the simplicity of the fully connected architecture limited its ability to account for spatial variations, potentially compromising prediction accuracy for high-contrast data.

In this work, we introduce a subspace-informed NO that learns to predict GMsFEM basis functions. Our key innovation is a hybrid approach that trains a NO to map heterogeneous fields to low-dimensional subspaces spanned by the GMsFEM basis functions. Rather than targeting individual basis functions—which can be sensitive to small perturbations—we design a subspace-aware loss function that enforces consistency with the governing physics at the subspace level. This shift in focus allows the NO to predict more stable and generalizable representations, even for high-contrast coefficients unseen during training.

We validate our method on two challenging benchmarks: a linear elliptic diffusion problem with sharp coefficient variations and the nonlinear steady-state Richards equation. Compared to standalone NOs, our approach reduces solution errors by approximately 60%, while cutting basis-construction time by  $60\times$  relative to classical GMsFEM. Crucially, our solver remains agnostic to forcing terms and boundary conditions, retaining the flexibility of NOs while inheriting the rigor of multiscale finite elements. By fusing the strengths of NOs (speed, adaptability) with GMsFEM (accuracy, interpretability), we deliver a practical tool for high-contrast PDEs.

Our main contributions are:

1. We introduce a novel hybrid approach that combines the strengths of NOs with GMsFEM (see Fig. 1).
2. We suggest a novel loss function to learn a linear subspace that significantly outperforms a standard  $L_2$  loss.
3. The approach is evaluated on high-contrast PDEs and shown to deliver better results than GMsFEM with a fraction of the computational cost.
4. Comparison with the standard protocol for training NOs shows that our hybrid approach is more accurate for in-distribution data and exhibits excellent out-of-distribution performance, which is infeasible with NOs without domain adaptation techniques.

## 2 GMsFEM+NO

### 2.1 Diffusion equation

We consider the diffusion equation with heterogeneous coefficients

$$-\nabla \cdot (\kappa(x)\nabla u(x)) = f(x), \quad x \in \Omega \equiv (0, 1)^2, \quad u(x)|_{x \in \partial\Omega} = 0, \quad (1)$$

where  $\partial\Omega$  is a boundary of the unit hypercube  $\Omega$ , and  $\kappa(x)$  is a heterogeneous field with high contrast. In particular, we assume that  $\kappa(x) \geq \varepsilon > 0$ , while  $\kappa(x)$  can have very large variations. For example, in this work we use  $\kappa(x)$  with values in range  $[1, 9600]$ .

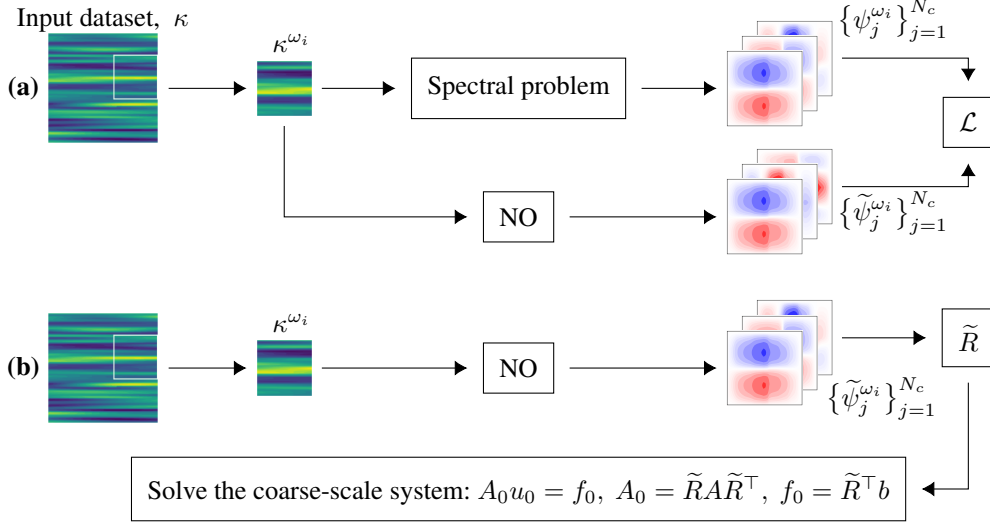


Figure 1: Illustration of training (a) and inference (b) stages of the proposed GMsFEM-NO method. NO is trained on heterogeneous fields  $\kappa^{\omega_i}$  that defined on subdomain  $\omega_i$  to predict subspace of basis functions  $\{\psi_j^{\omega_i}\}_{j=1}^{N_c}$ . During training the subspace-informed loss  $\mathcal{L}$  is applied to align predicted subspace  $\{\tilde{\psi}_j^{\omega_i}\}_{j=1}^{N_c}$  with  $\{\psi_j^{\omega_i}\}_{j=1}^{N_c}$ . During inference stage (b), the predicted subspace forms the matrix  $\tilde{R}$  that projects matrix  $A$  and vectors to the coarse space.

## 2.2 Steady-State Richards' equation

The steady-state version of Richards' equation, describing water movement in unsaturated porous media. The equation takes the form:

$$-\nabla \cdot (\kappa(x, u(x)) \nabla u(x)) = f(x), \quad x \in \Omega \equiv (0, 1)^2, \quad u(x)|_{x \in \partial\Omega} = 0, \quad (2)$$

where  $\kappa(x, u(x))$  is unsaturated hydraulic conductivity,  $u(x)$  is the water pressure and  $f(x)$  is a source or sink term.

We consider the Haverkamp model Haverkamp et al. [1977] to define  $\kappa(x, u(x))$ :

$$\kappa(x, u(x)) = K_s(x) K_r(u(x)) = \kappa(x) \frac{1}{1 + |u|},$$

where  $\kappa(x)$  is a heterogeneous field with high contrast that denotes the permeability of soils,  $K_r(u)$  represents the relative hydraulic conductivity,  $K_s(x)$  stands for the saturated hydraulic conductivity. All the multiscale heterogeneity is incorporated in  $\kappa(x)$  without regard to  $u$ , and  $\frac{1}{1 + |u|}$  includes all the non-linearity.

## 2.3 Generalized Multiscale Finite Element Method

### 2.3.1 Multiscale space approximation

Multiscale methods Efendiev and Hou [2009] form a broad class of numerical techniques. They are based on constructing multiscale basis functions in local domains to capture fine-scale behavior.

Let  $\mathcal{T}_H$  be a coarse mesh of the domain  $\Omega \subset \mathbb{R}^2$ :  $\mathcal{T}_H = \bigcup_{i=1}^N K_i$ , where  $K_i$  is the coarse cell, and  $N$  is the number of coarse cells. We denote by  $\{x_i\}_{i=1}^{N_v}$  the nodes of the coarse mesh  $\mathcal{T}_H$ , where  $N_v$  is the number of nodes of the coarse mesh. Let  $\omega_i$  be the subdomain defined as the collection of coarse cells containing the coarse grid node  $x_i$  (see Fig. 2):

$$\omega_i = \bigcup_j \{K_j \in \mathcal{T}_H : x_i \in \bar{K}_j\}.$$

To build a basis that ensures accurate approximations on the coarse mesh  $\mathcal{T}_H$ , we will derive spectral multiscale basis functions following the framework of the Generalized Multiscale Finite Element Method (GMsFEM).

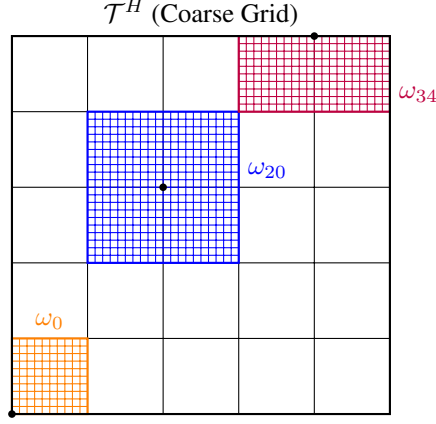


Figure 2: Illustration of the  $5 \times 5$  coarse grid  $\mathcal{T}_H$  with local domains  $(\omega_0, \omega_{20}, \omega_{34})$  that are denoted as corner (1 cell, e.g.,  $\omega_0$ ), half (2 cells, e.g.,  $\omega_{34}$ ), or full (4 cells, e.g.,  $\omega_{20}$ ) based on their coarse-cell count.

GMsFEM contains two stages:

- **Offline stage:**

1. Define coarse grid  $\mathcal{T}_H$  and generate local domains  $\omega_i$ ,  $i = 1, \dots, N_v$ ;
2. Construct the multiscale space  $\text{span}\{\psi_j^{\omega_i}\}_{j=1}^{N_c}$  by solving local spectral problems in each domain  $\omega_i$ , where  $N_c$  is the number of coarse basis functions, and multiplying the eigenvectors by partition of unity functions  $\chi_i$  Babuska and Lipton [2011], Babuška et al. [2008], Strouboulis et al. [2000];
3. Map the local degrees of freedom to global and form a restriction matrix  $R$  using a given number of  $N_{\text{bf}} \leq N_c$  local multiscale basis functions over each subdomain  $\omega_i$ .

- **Online stage:**

1. Project matrices and vectors to the coarse grid using the restriction matrix  $R$ ;
2. Solve the coarse-scale system;
3. Interpolate the coarse-scale solution to the fine grid resolution.

### 2.3.2 Spectral problem

Let  $\mathcal{T}_h$  be a fine grid, which is a refinement of  $\mathcal{T}_H$ , where  $h \ll H$ . We denote by  $V^h(\Omega)$  the usual finite element discretization of piecewise linear continuous functions with respect to the fine grid  $\mathcal{T}_h$ . For each local domain  $\omega_i$ , we define the Neumann matrix  $A_h^{\omega_i}$  by

$$v_h^\top A_h^{\omega_i} w_h = \int_{\omega_i} \kappa(x) \nabla v_h \cdot \nabla w_h \, dx, \quad \forall v_h, w_h \in V^h(\omega_i)$$

and the Mass matrix  $S_h^{\omega_i}$  by

$$v_h^\top S_h^{\omega_i} w_h = \int_{\omega_i} \kappa(x) v_h w_h \, dx, \quad \forall v_h, w_h \in V^h(\omega_i)$$

We consider the finite dimensional symmetric eigenvalue problem

$$A_h^{\omega_i} \phi = \lambda S_h^{\omega_i} \phi$$

and denote its eigenvalues and eigenvectors by  $\{\lambda^{\omega_i}\}_{j=1}^{N_c}$  and  $\{\phi^{\omega_i}\}_{j=1}^{N_c}$ , respectively. Note that  $\lambda_1^{\omega_i} = 0$  (corresponds to the constant eigenvector  $\phi_1^{\omega_i} = \text{const}$ ). We order eigenvalues as

$$\lambda_1^{\omega_i} \leq \lambda_2^{\omega_i} \leq \dots \leq \lambda_j^{\omega_i} \leq \dots$$

The eigenvectors  $\{\phi^{\omega_i}\}_{j=1}^{N_c}$  form an  $S_h^{\omega_i}$ -orthonormal basis of  $V^h(\omega_i)$ .

### 2.3.3 Solving of the coarse-scale system

For each local domain  $\omega_i$ , we select eigenvectors corresponding to the  $N_{\text{bf}} \leq N_c$  smallest eigenvalues and define a multiscale subspace

$$V_0 = \text{span}\{\psi_j^{\omega_i} = \chi_i \phi_j^{\omega_i} \mid j = 1, \dots, N_{\text{bf}}, i = 1, \dots, N_v\}.$$

and define the restriction matrix

$$R = [\psi_1^{\omega_1}, \dots, \psi_{N_{\text{bf}}}^{\omega_1}, \dots, \psi_1^{\omega_{N_v}}, \dots, \psi_{N_{\text{bf}}}^{\omega_{N_v}}]^\top.$$

Coarse-grid solution is the finite element projection of the fine-scale solution into the space  $V_0$ . More precisely, multiscale solution  $u_0$  is given by

$$A_0 u_0 = f_0,$$

where  $A_0 = RAR^\top$  is the projected system matrix,  $f_0 = R^\top b$  is projected right-hand side. The reconstructed fine-scale solution is  $u = R^\top u_0$ .

## 2.4 Neural Operator

Here we consider one type of NO that employs Fourier modes, but there are no restrictions on using other types of NOs. Fourier neural operators (FNOs) are a class of NOs motivated by Fourier spectral methods. Originally, Li et al. [2020] formulate each operator layer as

$$\mathcal{L}^\ell(z^{(\ell)}) = \sigma[W^{(\ell)}z^{(\ell)} + b^{(\ell)} + \mathcal{K}^{(\ell)}(z^{(\ell)})], \quad (3)$$

where  $W^{(\ell)}z^{(\ell)} + b^{(\ell)}$  is an affine point-wise map,

$$\mathcal{K}^{(\ell)}(z^{(\ell)}) = \text{IFFT}(\mathcal{R}^{(\ell)} \cdot \text{FFT}(z))$$

is a kernel integral operator. The Fourier domain weight matrices  $\{\mathcal{R}^{(\ell)}\}_{\ell=1}^L$  require  $O(LH^2MD)$  parameters, where  $H$  is the hidden size,  $M$  is the number of the top Fourier modes that are kept, and  $D$  is the dimension of the problem.

In Factorised FNO (FFNO) Tran et al. [2021], the operator layer in (3) is changed

$$\mathcal{L}^\ell(z^{(\ell)}) = z^{(\ell)} + \sigma[W_2^{(\ell)}\sigma(W_1^{(\ell)}\mathcal{K}^{(\ell)}(z^{(\ell)}) + b_1^{(\ell)}) + b_2^{(\ell)}],$$

where  $\mathcal{K}^{(\ell)}(z^{(\ell)}) = \sum_{d \in D} [\text{IFFT}(\mathcal{R}_d^{(\ell)} \cdot \text{FFT}_d(z^{(\ell)}))]$ . For this case, the number of parameters is  $O(LH^2MD)$ . Therefore, the FFNO allows to reduce the model complexity and allow it to scale to deeper networks.

## 2.5 Proposed method

### 2.5.1 Algorithm

We propose an efficient method for generating basis functions in the GMsFEM using NOs. Traditionally, the offline stage of GMsFEM requires solving an eigenvalue problem for each subdomain  $\omega_i$ , which is computationally expensive. Instead, we leverage NOs to predict multiple basis functions rapidly, significantly accelerating the offline phase.

Subdomains vary in shape and orientation (see Fig. 2), where orientation refers to the relative placement of the coarse node  $x_i$  shared by all cells in the subdomain. To address this variability, we categorize all local domains into three distinct groups: **full**, **corner**, and **half**. Before training, we normalize the orientation of each local domain by rotating both the input data and the target basis functions, ensuring a standardized coarse node  $x_i$  position within each group. This preprocessing step guarantees consistency in the input structure for the NO.

We train three separate NOs, each specialized for one domain group (see Fig. 3 (a-c)). Each NO predicts  $N_{\text{bf}}$  basis functions for subdomains within its assigned category (full, half, corner). This group-specific approach improves prediction accuracy by accounting for geometric variations across subdomain types.

For test data, we first decompose the computational domain into coarse subdomains and apply the necessary rotations to align input data with one of the predefined groups. The corresponding NO then generates the required basis functions. The predicted basis functions are extended to the domain  $\Omega$  (with zeros padded outside their respective subdomains) and vectorized to construct the restriction matrix  $R$ . Finally, the online stage of GmsFEM is executed to compute the multiscale solution.

This approach substantially reduces offline computational costs while maintaining the accuracy and flexibility of GmsFEM, making it particularly suitable for problems with heterogeneous or highly varying coefficients.

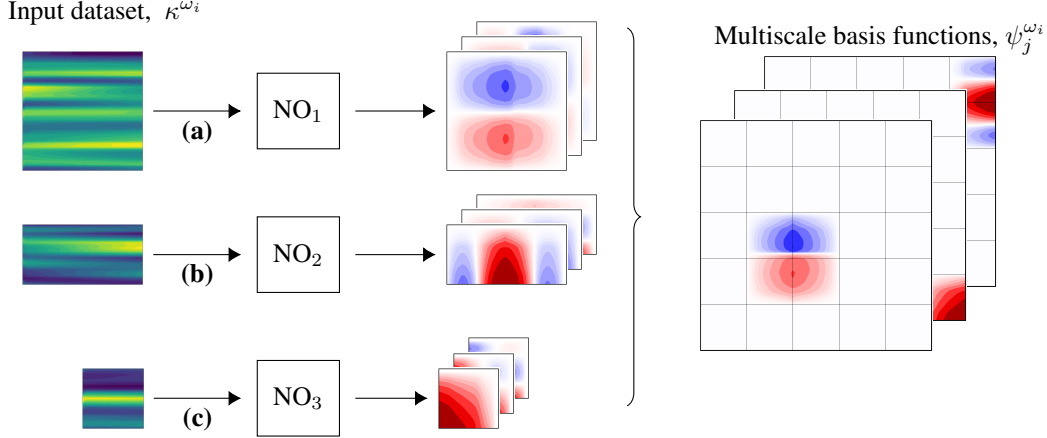


Figure 3: Multiscale basis generation algorithm for three subdomain types  $\omega_i$ : **(a) full**, **(b) half**, **(c) corner** - using dedicated NOs per type with further extension to  $\Omega$ .

### 2.5.2 Subspace-informed loss functions

The selection of an appropriate loss function is critical when training NOs to predict basis functions. A conventional loss function is  $L_2$  loss. Since basis functions are defined only up to their sign, the conventional  $L_2$  loss is adapted to account for this invariance, resulting in the Relative Basis Function  $L_2$  Loss (RBFL<sub>2</sub>):

$$\mathcal{L}_{\text{RBFL}_2} = \mathbb{E}_{i,j} \left[ \min \left( \frac{\|\psi_j^i - \tilde{\psi}_j^i\|_2^2}{\|\psi_j^i\|_2^2}, \frac{\|\psi_j^i + \tilde{\psi}_j^i\|_2^2}{\|\psi_j^i\|_2^2} \right) \right], \quad (4)$$

where  $\psi_j^i$  and  $\tilde{\psi}_j^i$  denote the  $j$ -th target and predicted basis functions for the  $i$ -th subdomain  $\omega_i$ , respectively. The minimization over  $\pm \tilde{\psi}_j^i$  ensures invariance to sign permutations, addressing the non-uniqueness of basis function orientations. While this loss improves robustness to sign variability, it remains fundamentally limited by its focus on individual basis functions rather than the subspace.

To address this, we propose a **Subspace Alignment Loss (SAL)** that directly optimizes the geometric consistency of the learned subspaces. Let  $R^i = [\psi_1^i, \dots, \psi_{N_{\text{bf}}}^i]^\top$  represent the target subspace basis and  $\tilde{R}^i$  denote the predicted subspace. The SAL measures alignment between subspaces using their orthonormalized bases  $Q_{R^i}$  and  $Q_{\tilde{R}^i}$ :

$$\mathcal{L}_{\text{SAL}} = \mathbb{E}_i \left[ N_{\text{bf}} - \|Q_{R^i}^\top Q_{\tilde{R}^i}\|_F^2 \right], \quad (5)$$

where the Frobenius norm term  $\|Q_{R^i}^\top Q_{\tilde{R}^i}\|_F^2$  quantifies the subspace overlap, achieving its maximum value  $N_{\text{bf}}$  when subspaces are perfectly aligned.

While SAL ensures subspace coherence, it may overlook finer discrepancies in how functions are projected onto the subspaces. To enforce consistency in projection behavior, we introduce a **Projection Regularization** term. This term evaluates the discrepancy between projections of a

randomized test vector  $v^i$  onto the target and predicted subspaces, governed by their projection matrices  $P_{R^i}$  and  $P_{\tilde{R}^i}$ :

$$\mathcal{L}_{\text{SAL-PR}} = \mathbb{E}_i \left[ \left( N_{\text{bf}} - \|Q_{R^i}^\top Q_{\tilde{R}^i}\|_F^2 \right) + \lambda \cdot \mathbb{E}_{c \sim \mathcal{N}(0, I)} \left\| (P_{R^i} - P_{\tilde{R}^i}) v^i \right\|_2^2 \right], \quad v^i = \sum_{k=1}^{N_{\text{bf}}} c_k \psi_k^i, \quad (6)$$

where  $P_{R^i} = Q_{R^i} Q_{R^i}^\top$ ,  $P_{\tilde{R}^i} = Q_{\tilde{R}^i} Q_{\tilde{R}^i}^\top$ ,  $\lambda$  is a hyperparameter set equal to 0.1.

### 3 Results

#### 3.1 Training details

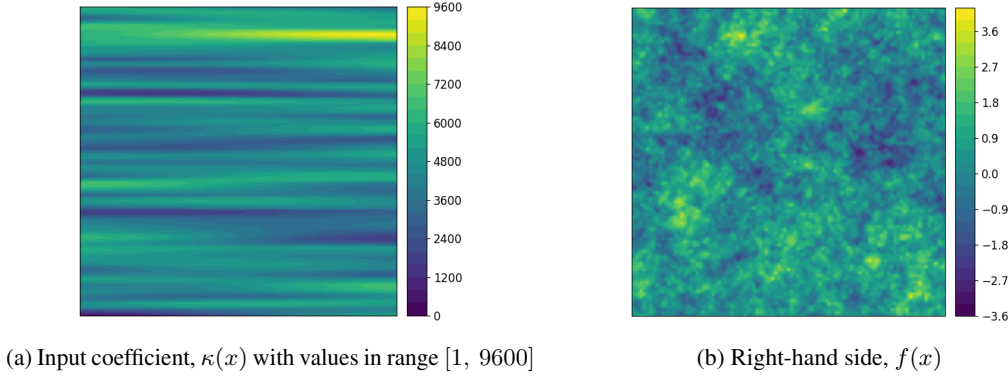


Figure 4: Example of input coefficient and right-hand side.

The study employs a dataset comprising  $100 \times 100$  resolution input coefficients (see Fig. 4a) for both Richards' equation and the elliptic equation. The computational domain  $\Omega$  is partitioned into 36 subdomains  $\omega_i$ , corresponding to a  $5 \times 5$  coarse-grid. The complete dataset contains 1000 samples, divided into training  $\mathcal{D}_{\text{train}}$  (800 samples) and testing  $\mathcal{D}_{\text{test}}$  (200 samples) datasets. Three distinct subdomain types contains different number of instances per one sample: 16 instances for **full** and **half**, 4 instances for **corner**. This distribution results in training datasets containing 4 times more samples for full and half subdomains than for corner-type subdomains. For training NOs, we utilized the first 4 and 8 basis functions ( $N_{\text{bf}}$ ) per subdomain as training targets.

To evaluate method robustness, we consider two right-hand side configurations:

- Uniform unit forcing term

$$f(x) = 1. \quad (7)$$

- Spatially variable forcing (see Fig. 4b) defined by

$$f(x) \sim \gamma \cdot \mathcal{N}(\alpha \cdot (I - \Delta)^{-\beta}), \quad \gamma = 2000, \alpha = 1, \beta = 0.5. \quad (8)$$

To measure quality of the obtained solutions on fine grid, we use the following metrics:

$$L_2 = \mathbb{E}_n \left[ \sqrt{\frac{\int_{\Omega} |u_h^n - \tilde{u}_h^n|^2 dx}{\int_{\Omega} |u_h^n|^2 dx}} \right], \quad H_1 = \mathbb{E}_n \left[ \sqrt{\frac{\int_{\Omega} |\nabla u_h^n - \nabla \tilde{u}_h^n|^2 dx}{\int_{\Omega} |\nabla u_h^n|^2 dx}} \right].$$

All experiments were performed on a single Nvidia Tesla H100 80Gb HBM3. Depending on the architecture and loss function training time is in-between 20 and 150 minutes for one NO.

#### 3.2 $\mathcal{L}_{\text{RBFL}_2}$ vs. $\mathcal{L}_{\text{SAL}}$ , $\mathcal{L}_{\text{SAL-PR}}$

To determine the optimal training configuration for the NOs tasked with predicting basis function subspaces, we conducted a grid search over key parameters. These included architectural parameters

(e.g., number of layers, modes, and hidden layer features) and training hyperparameters (e.g., batch size, loss function type). Detailed specifications for all parameters except the loss function type are provided in Appendix A. The results for the different losses are shown in Table 1.

As shown in Table 1,  $\mathcal{L}_{\text{RBFL}_2}$  underperforms compared to our proposed subspace alignment losses ( $\mathcal{L}_{\text{SAL}}$ ,  $\mathcal{L}_{\text{SAL-PR}}$ ). For the Richards equation with complex right-hand side (8) and 4 basis functions, our proposed loss improves the relative  $L_2$  metric by a factor of 1.6. For the Richards equation with simple right-hand side (7) and 8 basis functions, our proposed loss improves the relative  $L_2$  metric by a factor of 1.8. Notably, the projection regularization term in  $\mathcal{L}_{\text{SAL-PR}}$  yielded nearly identical results to  $\mathcal{L}_{\text{SAL}}$ . The minimal impact of projection regularization may stem from the relatively small grid resolution: in smaller grids, the subspace alignment term alone suffices to capture dominant features of the basis functions subspace.

Table 1: The comparison of different loss functions used for NO training.

$N_{\text{bf}}$	Dataset	$\mathcal{L}_{\text{RBFL}_2}$		$\mathcal{L}_{\text{SAL}}$		$\mathcal{L}_{\text{SAL-PR}}$	
		$L_2$	$H_1$	$L_2$	$H_1$	$L_2$	$H_1$
4	Diffusion, (7)	2.72%	19.10%	<b>2.39%</b>	18.01%	2.40%	18.01%
	Diffusion, (8)	6.03%	29.10%	<b>5.76%</b>	28.40%	5.78%	28.43%
	Richards, (7)	3.87%	16.26%	<b>3.14%</b>	15.01%	3.17%	15.02%
	Richards, (8)	9.78%	34.39%	<b>6.11%</b>	29.37%	6.13%	29.42%
8	Diffusion, (7)	1.75%	14.83%	<b>1.06%</b>	11.57%	<b>1.06%</b>	11.65%
	Diffusion, (8)	3.53%	21.77%	2.82%	19.07%	<b>2.81%</b>	19.03%
	Richards, (7)	3.46%	15.04%	1.88%	11.10%	<b>1.87%</b>	11.25%
	Richards, (8)	3.77%	22.38%	<b>2.99%</b>	19.61%	<b>2.99%</b>	19.60%

### 3.3 GMsFEM vs. GMsFEM-NO

In this section, we compare the performance of the original GMsFEM and our proposed GMsFEM-NO method in terms of solution accuracy (quantified by  $L_2$  and  $H_1$  metrics) and computational efficiency for basis function generation.

As shown in Table 2, GMsFEM-NO achieves marginally better  $L_2$  and  $H_1$  errors than GMsFEM across all datasets and basis function counts ( $N_{\text{bf}}$ ). This improvement may seem counterintuitive since GMsFEM-NO is trained on GMsFEM-generated basis functions. The enhancement can be attributed to the NO’s ability to learn a low-dimensional subspace spanning the original basis functions rather than replicating them directly. By enforcing global structural coherence through the subspace alignment loss, redundancies are reduced, and the subspace’s representational efficiency is enhanced.

Table 3 compares the time required to generate 4 and 8 basis functions using the GMsFEM offline stage and GMsFEM-NO (which employs three NOs, one for each subdomain type). The proposed method achieves a  $50\times$  speedup for  $N_{\text{bf}} = 4$  and  $60\times$  speedup for  $N_{\text{bf}} = 8$ , demonstrating its computational superiority.

### 3.4 NO vs. GMsFEM-NO

In this section, we compare the performance of the proposed GMsFEM-NO framework against a standalone NO trained to directly predict PDE solutions. While the standalone NO offers faster inference and might achieve comparable accuracy, its performance deteriorates significantly for high-dimensional, high-contrast datasets. We validate this through empirical testing (full training details are provided in the Appendix B).

As shown in Table 4, GMsFEM-NO achieves lower relative  $L_2$  errors compared to the standalone NO across all datasets. For instance, when applied to Richards’ equation with the complex right-hand side defined in (8), GMsFEM-NO demonstrates a  $1.7\times$  reduction in the relative  $L_2$  error compared to the standalone NO.

Table 2: The comparison of results obtained by GMsFEM and proposed GMsFEM-NO methods.

$N_{\text{bf}}$	Dataset	GMsFEM		GMsFEM-NO	
		$L_2$	$H_1$	$L_2$	$H_1$
4	Diffusion, (7)	2.49%	18.27%	<b>2.39%</b>	18.01%
	Diffusion, (8)	5.91%	29.30%	<b>5.76%</b>	28.40%
	Richards, (7)	3.30%	15.45%	<b>3.14%</b>	15.01%
	Richards, (8)	7.31%	32.05%	<b>6.11%</b>	29.37%
8	Diffusion, (7)	1.15%	11.68%	<b>1.06%</b>	11.57%
	Diffusion, (8)	2.82%	19.07%	<b>2.81%</b>	19.03%
	Richards, (7)	2.03%	11.68%	<b>1.87%</b>	11.25%
	Richards, (8)	3.09%	20.20%	<b>2.99%</b>	19.60%

Table 3: The comparison of time needed for basis functions generation using GMsFEM-NO and GMsFEM offline stage.

$N_{\text{bf}}$	GMsFEM, sec.	GMsFEM-NO, sec.
4	14.35	<b>0.27</b>
8	16.87	<b>0.28</b>

A critical advantage of GMsFEM-NO over the standalone NO lies in its independence from the right-hand side terms of the PDE. The standalone NO exhibits catastrophic failure when tested on out-of-distribution forcing terms, as evidenced in Table 5. Retraining the NO for new right-hand side terms requires computationally expensive recalculation of solutions, highlighting a key limitation of standalone NO learning.

Table 4: The comparison of relative  $L_2$  error for solutions obtained by NO and by GMsFEM-NO.

Dataset	NO	GMsFEM-NO
Diffusion, (7)	1.68%	<b>1.06%</b>
Diffusion, (8)	4.07%	<b>2.81%</b>
Richards, (7)	3.07%	<b>1.87%</b>
Richards, (8)	5.16%	<b>2.99%</b>

Table 5: Out-of-distribution results for the NO: training and testing on PDEs with different right-hand sides.

Train, $\mathcal{D}_{\text{train}}$	Test, $\mathcal{D}_{\text{test}}$	$L_2$
Diffusion, (7)	Diffusion, (8)	228%
Diffusion, (8)	Diffusion, (7)	988%
Richards, (7)	Richards, (8)	248%
Richards, (8)	Richards, (7)	2311%

## 4 Conclusion

In this work, we propose the GMsFEM-NO method for solving PDEs. This approach employs NOs during the offline stage of GMsFEM to predict basis function subspaces, replacing the conventional eigenvalue problem solution. We tested the proposed method on standard multiscale benchmarks: a linear elliptic diffusion problem and the nonlinear steady-state version of Richards equation. GMsFEM-NO achieves a  $60\times$  speedup in basis generation compared to the GMsFEM basis

generation. Another key contribution is our novel subspace alignment loss, which enables learning of the subspace of basis functions, improving the  $L_2$  metric by factors of 1.6 – 1.8 compared to conventional  $\mathcal{L}_{\text{RBF}L_2}$  loss. Notably, GMSFEM-NO demonstrates superior robustness to standalone NOs, reducing errors by  $1.7\times$  on high-contrast problems. Furthermore, the GMSFEM-NO offline stage remains independent of the PDE’s right-hand side. Thus, while standalone NOs exhibit over 200%  $L_2$  error on out-of-distribution data, our approach maintains consistent performance across varying forcing terms. By preserving the mathematical structure of multiscale methods while leveraging NO speed, this work establishes a practical paradigm for heterogeneous PDE simulation.

The primary limitation of our method is its current restriction to structured grids due to the chosen NO architecture. Additionally, our experiments focused on relatively small grid sizes, which may not fully represent large-scale applications. The study was also limited to two time-independent equation types with Dirichlet boundary conditions.

Future work should address more complex PDE types, including time-dependent formulations of applied interest. More research is needed on finer grid resolutions and the influence of coarse grid sizing. Furthermore, future work should involve developing grid-agnostic architectures, such as graph neural operators, to efficiently handle irregular domains and complex geometries inherent to real-world applications.

## References

- Kamyar Azizzadenesheli, Nikola Kovachki, Zongyi Li, Miguel Liu-Schiaffini, Jean Kossaifi, and Anima Anandkumar. Neural operators for accelerating scientific simulations and design. *Nature Reviews Physics*, 6(5):320–328, 2024.
- George Em Karniadakis, Ioannis G Kevrekidis, Lu Lu, Paris Perdikaris, Sifan Wang, and Liu Yang. Physics-informed machine learning. *Nature Reviews Physics*, 3(6):422–440, 2021.
- Nikola Kovachki, Zongyi Li, Burigede Liu, Kamyar Azizzadenesheli, Kaushik Bhattacharya, Andrew Stuart, and Anima Anandkumar. Neural operator: Learning maps between function spaces with applications to pdes. *Journal of Machine Learning Research*, 24(89):1–97, 2023.
- Zongyi Li, Nikola Kovachki, Kamyar Azizzadenesheli, Burigede Liu, Kaushik Bhattacharya, Andrew Stuart, and Anima Anandkumar. Fourier neural operator for parametric partial differential equations. *arXiv preprint arXiv:2010.08895*, 2020.
- Alasdair Tran, Alexander Mathews, Lexing Xie, and Cheng Soon Ong. Factorized fourier neural operators. *arXiv preprint arXiv:2111.13802*, 2021.
- Lu Lu, Pengzhan Jin, and George Em Karniadakis. Deeponet: Learning nonlinear operators for identifying differential equations based on the universal approximation theorem of operators. *arXiv preprint arXiv:1910.03193*, 2019.
- Yalchin Efendiev, Juan Galvis, and Xiao-Hui Wu. Multiscale finite element methods for high-contrast problems using local spectral basis functions. *Journal of Computational Physics*, 230(4):937–955, 2011.
- Yalchin Efendiev, Juan Galvis, and Thomas Y Hou. Generalized multiscale finite element methods (gmsfem). *Journal of computational physics*, 251:116–135, 2013.
- Eric T Chung, Yalchin Efendiev, Guanglian Li, and Maria Vasilyeva. Generalized multiscale finite element methods for problems in perforated heterogeneous domains. *Applicable Analysis*, 95(10):2254–2279, 2016.
- Denis Spiridonov, Sergei Stepanov, and Tina Mai. Prediction of discretization of online gmsfem using deep learning for richards equation. *Journal of Computational and Applied Mathematics*, 454:116167, 2025.
- Lorenzo Adolph Richards. Capillary conduction of liquids through porous mediums. *physics*, 1(5):318–333, 1931.
- Matthew W Farthing and Fred L Ogden. Numerical solution of richards’ equation: A review of advances and challenges. *Soil Science Society of America Journal*, 81(6):1257–1269, 2017.

- Roland Haverkamp, Michel Vauclin, Jaoudat Touma, PJ Wierenga, and Georges Vachaud. A comparison of numerical simulation models for one-dimensional infiltration. *Soil Science Society of America Journal*, 41(2):285–294, 1977.
- Yalchin Efendiev and Thomas Y Hou. *Multiscale finite element methods: theory and applications*, volume 4. Springer Science & Business Media, 2009.
- Ivo Babuska and Robert Lipton. Optimal local approximation spaces for generalized finite element methods with application to multiscale problems. *Multiscale Modeling & Simulation*, 9(1):373–406, 2011.
- Ivo Babuška, Victor Nistor, and Nicolae Tarfulea. Generalized finite element method for second-order elliptic operators with dirichlet boundary conditions. *Journal of Computational and Applied Mathematics*, 218(1):175–183, 2008.
- Theofanis Strouboulis, Ivo Babuška, and Kevin Copps. The design and analysis of the generalized finite element method. *Computer methods in applied mechanics and engineering*, 181(1-3):43–69, 2000.
- Ilya Loshchilov and Frank Hutter. Decoupled weight decay regularization. *arXiv preprint arXiv:1711.05101*, 2017.
- DeepMind, Igor Babuschkin, Kate Baumli, Alison Bell, Surya Bhupatiraju, Jake Bruce, Peter Buchlovsky, David Budden, Trevor Cai, Aidan Clark, Ivo Danihelka, Antoine Dedieu, Claudio Fantacci, Jonathan Godwin, Chris Jones, Ross Hemsley, Tom Hennigan, Matteo Hessel, Shaobo Hou, Steven Kapturowski, Thomas Keck, Iurii Kemaev, Michael King, Markus Kunesch, Lena Martens, Hamza Merzic, Vladimir Mikulik, Tamara Norman, George Papamakarios, John Quan, Roman Ring, Francisco Ruiz, Alvaro Sanchez, Laurent Sartran, Rosalia Schneider, Eren Sezener, Stephen Spencer, Srivatsan Srinivasan, Miloš Stanojević, Wojciech Stokowiec, Luyu Wang, Guangyao Zhou, and Fabio Viola. The DeepMind JAX Ecosystem, 2020. URL <http://github.com/google-deepmind>.
- Patrick Kidger and Cristian Garcia. Equinox: neural networks in JAX via callable PyTrees and filtered transformations. *Differentiable Programming workshop at Neural Information Processing Systems 2021*, 2021.
- Xiangning Chen, Chen Liang, Da Huang, Esteban Real, Kaiyuan Wang, Hieu Pham, Xuanyi Dong, Thang Luong, Cho-Jui Hsieh, Yifeng Lu, et al. Symbolic discovery of optimization algorithms. *Advances in neural information processing systems*, 36:49205–49233, 2023.

## A GMSFEM-NO Training Details

Table 6: GMSFEM-NO training details for (7),  $N_{bf} = 4$ .

Loss	Subdomain type	$N_{batch}$	$N_{modes}$	$N_{layers}$
(4)	<b>full</b>	32	16, 16	5
	<b>half</b>	32	14, 8	5
	<b>corner</b>	32	6, 6	5
(5)	<b>full</b>	32	16, 16	5
	<b>half</b>	32	8, 8	5
	<b>corner</b>	32	6, 6	5
(6)	<b>full</b>	32	16, 16	4
	<b>half</b>	32	14, 8	4
	<b>corner</b>	32	10, 10	4

Table 7: GMSFEM-NO training details for (8),  $N_{\text{bf}} = 4$ .

Loss	Subdomain type	$N_{\text{batch}}$	$N_{\text{modes}}$	$N_{\text{layers}}$
(4)	<b>full</b>	32	16, 16	5
	<b>half</b>	32	8, 8	5
	<b>corner</b>	32	10, 10	5
(5)	<b>full</b>	32	16, 16	5
	<b>half</b>	32	8, 8	5
	<b>corner</b>	32	6, 6	5
(6)	<b>full</b>	32	16, 16	4
	<b>half</b>	32	14, 8	4
	<b>corner</b>	32	10, 10	4

Table 8: GMSFEM-NO training details for (7),  $N_{\text{bf}} = 8$ .

Loss	Subdomain type	$N_{\text{batch}}$	$N_{\text{modes}}$	$N_{\text{layers}}$
(4)	<b>full</b>	16	18, 18	5
	<b>half</b>	16	14, 8	5
	<b>corner</b>	16	8, 8	5
(5)	<b>full</b>	16	16, 16	5
	<b>half</b>	16	10, 10	5
	<b>corner</b>	16	8, 8	5
(6)	<b>full</b>	32	18, 18	5
	<b>half</b>	32	14, 8	5
	<b>corner</b>	32	10, 10	5

Table 9: GMSFEM-NO training details for (8),  $N_{\text{bf}} = 8$ .

Loss	Subdomain type	$N_{\text{batch}}$	$N_{\text{modes}}$	$N_{\text{layers}}$
(4)	<b>full</b>	16	18, 18	5
	<b>half</b>	16	14, 8	5
	<b>corner</b>	16	8, 8	5
(5)	<b>full</b>	16	16, 16	5
	<b>half</b>	16	10, 10	5
	<b>corner</b>	16	8, 8	5
(6)	<b>full</b>	32	18, 18	5
	<b>half</b>	32	14, 8	5
	<b>corner</b>	32	10, 10	5

For FFNO training to predict basis functions subspace, we used AdamW optimizer Loshchilov and Hutter [2017] with cosine decay learning rate scheduler. The initial learning rate was  $10^{-4}$ . We trained NO for 800 epochs. For the rest of the hyperparameters, we performed a grid search:

1. Batch size  $[8, 16, 32]$ .
2. Number of operator layers  $[4, 5]$ .

Table 10: GMsFEM-NO training details for (7),  $N_{\text{bf}} = 4$ .

Loss	Subdomain type	$N_{\text{batch}}$	$N_{\text{modes}}$	$N_{\text{layers}}$
(4)	<b>full</b>	32	16, 16	5
	<b>half</b>	32	8, 8	5
	<b>corner</b>	32	10, 10	5
(5)	<b>full</b>	32	16, 16	5
	<b>half</b>	32	8, 8	5
	<b>corner</b>	32	6, 6	5
(6)	<b>full</b>	32	16, 16	4
	<b>half</b>	32	14, 8	4
	<b>corner</b>	32	10, 10	4

Table 11: GMsFEM-NO training details for (8),  $N_{\text{bf}} = 4$ .

Loss	Subdomain type	$N_{\text{batch}}$	$N_{\text{modes}}$	$N_{\text{layers}}$
(4)	<b>full</b>	32	16, 16	5
	<b>half</b>	32	8, 8	5
	<b>corner</b>	32	10, 10	5
(5)	<b>full</b>	32	16, 16	5
	<b>half</b>	32	8, 8	5
	<b>corner</b>	32	6, 6	5
(6)	<b>full</b>	32	16, 16	4
	<b>half</b>	32	14, 8	4
	<b>corner</b>	32	10, 10	4

Table 12: GMsFEM-NO training details for (7),  $N_{\text{bf}} = 8$ .

Loss	Subdomain type	$N_{\text{batch}}$	$N_{\text{modes}}$	$N_{\text{layers}}$
(4)	<b>full</b>	32	18, 18	5
	<b>half</b>	32	14, 8	5
	<b>corner</b>	32	10, 10	5
(5)	<b>full</b>	16	16, 16	5
	<b>half</b>	16	10, 10	5
	<b>corner</b>	16	8, 8	5
(6)	<b>full</b>	32	18, 18	5
	<b>half</b>	32	14, 8	5
	<b>corner</b>	32	10, 10	5

3. Number of modes used in FFNO kernel:

- for full domains  $[[16, 16], [18, 18]]$ ;
- for half domains  $[[8, 8], [10, 10], [14, 8], [14, 10]]$ ;
- for corner domains  $[[6, 6], [8, 8], [10, 10]]$ .

4. Number of channels in the FFNO kernel  $[64, 128]$ .

Table 13: GMSFEM-NO training details for (8),  $N_{\text{bf}} = 8$ .

Loss	Subdomain type	$N_{\text{batch}}$	$N_{\text{modes}}$	$N_{\text{layers}}$
(4)	<b>full</b>	16	18, 18	5
	<b>half</b>	16	14, 8	5
	<b>corner</b>	16	10, 10	5
(5)	<b>full</b>	16	16, 16	5
	<b>half</b>	16	8, 8	5
	<b>corner</b>	16	8, 8	5
(6)	<b>full</b>	32	18, 18	5
	<b>half</b>	32	14, 8	5
	<b>corner</b>	32	10, 10	5

The optimal parameters, which vary depending on the loss function type, subdomain type, equation type, and forcing terms, can be found in Tables 6, 7, 8, 9, 10, 11, 12, 13. The optimal number of channels in the FFNO kernel is 128 for all NOs. We use JAX, Optax DeepMind et al. [2020] and Equinox Kidger and Garcia [2021] in all experiments.

## B NO Training Details

For FFNO Tran et al. [2021], we performed training with the following protocol. For all experiments, we used a Lion optimizer Chen et al. [2023] with exponential learning rate decay. The initial learning rate was  $10^{-4}$ , and the decay rate was set to 0.5. FFNO had 4 operator layers and the number of training epochs was 10000. We used 80% of the available data for training and the remaining 20% for evaluation. For the rest of the hyperparameters, we performed a grid search:

1. Batch size  $[10, 50, 100]$ .
2. Number of transition steps for exponential decay of learning rate  $[100, 200]$  measured in the number of epochs.
3. Number of modes used in FFNO kernel  $[12, 16]$ .
4. Number of channels in the FFNO kernel  $[32, 64]$ .

For each equation, in Table 4, we report the best relative test error reached with the hyperparameters tried. We also evaluated trained networks on out-of-distribution data but observed that the relative error exceeds 100%. The best hyperparameters are: a batch size of 100, 100 transition steps for exponential decay, 12 modes, and 64 channels.

## NeurIPS Paper Checklist

### 1. Claims

Question: Do the main claims made in the abstract and introduction accurately reflect the paper’s contributions and scope?

Answer: [\[Yes\]](#)

Justification: We made the following claims: (i) We introduce a novel hybrid approach that combines the strengths of neural operators (NOs) with the Generalized Multiscale Finite Element Method (GMsFEM). (ii) We propose a novel loss function for learning a linear subspace. (iii) This loss function significantly outperforms the standard  $L_2$  loss for GMsFEM-NO method. (iv) The GMsFEM-NO approach computes basis functions substantially faster than the original GMsFEM. (v) GMsFEM-NO surpasses standalone NO in terms of evaluation metrics and out-of-distribution performance.

All claims are supported by theoretical or experimental evidence: (i–ii) To the best of our knowledge, NOs have not previously been applied to predict the subspace of GMsFEM basis functions, particularly with a subspace-informed loss function. The closest related work is the study by Spiridonov et al. [2025], which employs a fully connected neural network to predict a single basis function for the steady-state Richards equation. (iii) The superiority of our loss function is demonstrated in Table 1. (iv) Computational efficiency is validated in Tables 2 and 3. (v) Comparative advantages over standalone NO are supported by the experimental results in Section 3.4.

Guidelines:

- The answer NA means that the abstract and introduction do not include the claims made in the paper.
- The abstract and/or introduction should clearly state the claims made, including the contributions made in the paper and important assumptions and limitations. A No or NA answer to this question will not be perceived well by the reviewers.
- The claims made should match theoretical and experimental results, and reflect how much the results can be expected to generalize to other settings.
- It is fine to include aspirational goals as motivation as long as it is clear that these goals are not attained by the paper.

### 2. Limitations

Question: Does the paper discuss the limitations of the work performed by the authors?

Answer: [\[Yes\]](#)

Justification: We explicitly discuss limitations in Section 4.

Guidelines:

- The answer NA means that the paper has no limitation while the answer No means that the paper has limitations, but those are not discussed in the paper.
- The authors are encouraged to create a separate "Limitations" section in their paper.
- The paper should point out any strong assumptions and how robust the results are to violations of these assumptions (e.g., independence assumptions, noiseless settings, model well-specification, asymptotic approximations only holding locally). The authors should reflect on how these assumptions might be violated in practice and what the implications would be.
- The authors should reflect on the scope of the claims made, e.g., if the approach was only tested on a few datasets or with a few runs. In general, empirical results often depend on implicit assumptions, which should be articulated.
- The authors should reflect on the factors that influence the performance of the approach. For example, a facial recognition algorithm may perform poorly when image resolution is low or images are taken in low lighting. Or a speech-to-text system might not be used reliably to provide closed captions for online lectures because it fails to handle technical jargon.
- The authors should discuss the computational efficiency of the proposed algorithms and how they scale with dataset size.

- If applicable, the authors should discuss possible limitations of their approach to address problems of privacy and fairness.
- While the authors might fear that complete honesty about limitations might be used by reviewers as grounds for rejection, a worse outcome might be that reviewers discover limitations that aren't acknowledged in the paper. The authors should use their best judgment and recognize that individual actions in favor of transparency play an important role in developing norms that preserve the integrity of the community. Reviewers will be specifically instructed to not penalize honesty concerning limitations.

### 3. Theory assumptions and proofs

Question: For each theoretical result, does the paper provide the full set of assumptions and a complete (and correct) proof?

Answer: [NA]

Justification: The paper is based on the well-developed theory of GMsFEM.

Guidelines:

- The answer NA means that the paper does not include theoretical results.
- All the theorems, formulas, and proofs in the paper should be numbered and cross-referenced.
- All assumptions should be clearly stated or referenced in the statement of any theorems.
- The proofs can either appear in the main paper or the supplemental material, but if they appear in the supplemental material, the authors are encouraged to provide a short proof sketch to provide intuition.
- Inversely, any informal proof provided in the core of the paper should be complemented by formal proofs provided in appendix or supplemental material.
- Theorems and Lemmas that the proof relies upon should be properly referenced.

### 4. Experimental result reproducibility

Question: Does the paper fully disclose all the information needed to reproduce the main experimental results of the paper to the extent that it affects the main claims and/or conclusions of the paper (regardless of whether the code and data are provided or not)?

Answer: [Yes]

Justification: We provide a detailed description of architectures, optimizers, and hyperparameters in Appendix A and B. Also, we describe dataset and train/test splits in Section 3.1. We will provide a link to the dataset and code if the paper is accepted to preserve anonymity.

Guidelines:

- The answer NA means that the paper does not include experiments.
- If the paper includes experiments, a No answer to this question will not be perceived well by the reviewers: Making the paper reproducible is important, regardless of whether the code and data are provided or not.
- If the contribution is a dataset and/or model, the authors should describe the steps taken to make their results reproducible or verifiable.
- Depending on the contribution, reproducibility can be accomplished in various ways. For example, if the contribution is a novel architecture, describing the architecture fully might suffice, or if the contribution is a specific model and empirical evaluation, it may be necessary to either make it possible for others to replicate the model with the same dataset, or provide access to the model. In general, releasing code and data is often one good way to accomplish this, but reproducibility can also be provided via detailed instructions for how to replicate the results, access to a hosted model (e.g., in the case of a large language model), releasing of a model checkpoint, or other means that are appropriate to the research performed.
- While NeurIPS does not require releasing code, the conference does require all submissions to provide some reasonable avenue for reproducibility, which may depend on the nature of the contribution. For example
  - (a) If the contribution is primarily a new algorithm, the paper should make it clear how to reproduce that algorithm.

- (b) If the contribution is primarily a new model architecture, the paper should describe the architecture clearly and fully.
- (c) If the contribution is a new model (e.g., a large language model), then there should either be a way to access this model for reproducing the results or a way to reproduce the model (e.g., with an open-source dataset or instructions for how to construct the dataset).
- (d) We recognize that reproducibility may be tricky in some cases, in which case authors are welcome to describe the particular way they provide for reproducibility. In the case of closed-source models, it may be that access to the model is limited in some way (e.g., to registered users), but it should be possible for other researchers to have some path to reproducing or verifying the results.

## 5. Open access to data and code

Question: Does the paper provide open access to the data and code, with sufficient instructions to faithfully reproduce the main experimental results, as described in supplemental material?

Answer: [No]

Justification: We will provide a link to the dataset and code if the paper is accepted to preserve anonymity.

Guidelines:

- The answer NA means that paper does not include experiments requiring code.
- Please see the NeurIPS code and data submission guidelines (<https://nips.cc/public/guides/CodeSubmissionPolicy>) for more details.
- While we encourage the release of code and data, we understand that this might not be possible, so “No” is an acceptable answer. Papers cannot be rejected simply for not including code, unless this is central to the contribution (e.g., for a new open-source benchmark).
- The instructions should contain the exact command and environment needed to run to reproduce the results. See the NeurIPS code and data submission guidelines (<https://nips.cc/public/guides/CodeSubmissionPolicy>) for more details.
- The authors should provide instructions on data access and preparation, including how to access the raw data, preprocessed data, intermediate data, and generated data, etc.
- The authors should provide scripts to reproduce all experimental results for the new proposed method and baselines. If only a subset of experiments are reproducible, they should state which ones are omitted from the script and why.
- At submission time, to preserve anonymity, the authors should release anonymized versions (if applicable).
- Providing as much information as possible in supplemental material (appended to the paper) is recommended, but including URLs to data and code is permitted.

## 6. Experimental setting/details

Question: Does the paper specify all the training and test details (e.g., data splits, hyperparameters, how they were chosen, type of optimizer, etc.) necessary to understand the results?

Answer: [Yes]

Justification: We provide a detailed description of architectures, optimizers, and hyperparameters in Appendix A and B. Also, we describe dataset and train/test splits in Section 3.1.

Guidelines:

- The answer NA means that the paper does not include experiments.
- The experimental setting should be presented in the core of the paper to a level of detail that is necessary to appreciate the results and make sense of them.
- The full details can be provided either with the code, in appendix, or as supplemental material.

## 7. Experiment statistical significance

Question: Does the paper report error bars suitably and correctly defined or other appropriate information about the statistical significance of the experiments?

Answer: [No]

Justification: Unfortunately, identifying the optimal hyperparameters required a significant amount of time. Therefore, there was insufficient time to perform cross-validation or conduct additional experiments to compute error bars for all results.

Guidelines:

- The answer NA means that the paper does not include experiments.
- The authors should answer "Yes" if the results are accompanied by error bars, confidence intervals, or statistical significance tests, at least for the experiments that support the main claims of the paper.
- The factors of variability that the error bars are capturing should be clearly stated (for example, train/test split, initialization, random drawing of some parameter, or overall run with given experimental conditions).
- The method for calculating the error bars should be explained (closed form formula, call to a library function, bootstrap, etc.)
- The assumptions made should be given (e.g., Normally distributed errors).
- It should be clear whether the error bar is the standard deviation or the standard error of the mean.
- It is OK to report 1-sigma error bars, but one should state it. The authors should preferably report a 2-sigma error bar than state that they have a 96% CI, if the hypothesis of Normality of errors is not verified.
- For asymmetric distributions, the authors should be careful not to show in tables or figures symmetric error bars that would yield results that are out of range (e.g. negative error rates).
- If error bars are reported in tables or plots, The authors should explain in the text how they were calculated and reference the corresponding figures or tables in the text.

## 8. Experiments compute resources

Question: For each experiment, does the paper provide sufficient information on the computer resources (type of compute workers, memory, time of execution) needed to reproduce the experiments?

Answer: [Yes]

Justification: All experiments were run on a single Nvidia Tesla H100 80Gb HBM3, this information is available in Section 3.1.

Guidelines:

- The answer NA means that the paper does not include experiments.
- The paper should indicate the type of compute workers CPU or GPU, internal cluster, or cloud provider, including relevant memory and storage.
- The paper should provide the amount of compute required for each of the individual experimental runs as well as estimate the total compute.
- The paper should disclose whether the full research project required more compute than the experiments reported in the paper (e.g., preliminary or failed experiments that didn't make it into the paper).

## 9. Code of ethics

Question: Does the research conducted in the paper conform, in every respect, with the NeurIPS Code of Ethics <https://neurips.cc/public/EthicsGuidelines>?

Answer: [Yes]

Justification: We carefully reviewed the NeurIPS Code of Ethics and confirmed that during the preparation of the research, we strictly followed all the guidelines.

Guidelines:

- The answer NA means that the authors have not reviewed the NeurIPS Code of Ethics.

- If the authors answer No, they should explain the special circumstances that require a deviation from the Code of Ethics.
- The authors should make sure to preserve anonymity (e.g., if there is a special consideration due to laws or regulations in their jurisdiction).

#### 10. **Broader impacts**

Question: Does the paper discuss both potential positive societal impacts and negative societal impacts of the work performed?

Answer: [NA]

Justification: The article is on the novel method GMsFEM-NO. It is mostly of interest to applied mathematics.

Guidelines:

- The answer NA means that there is no societal impact of the work performed.
- If the authors answer NA or No, they should explain why their work has no societal impact or why the paper does not address societal impact.
- Examples of negative societal impacts include potential malicious or unintended uses (e.g., disinformation, generating fake profiles, surveillance), fairness considerations (e.g., deployment of technologies that could make decisions that unfairly impact specific groups), privacy considerations, and security considerations.
- The conference expects that many papers will be foundational research and not tied to particular applications, let alone deployments. However, if there is a direct path to any negative applications, the authors should point it out. For example, it is legitimate to point out that an improvement in the quality of generative models could be used to generate deepfakes for disinformation. On the other hand, it is not needed to point out that a generic algorithm for optimizing neural networks could enable people to train models that generate Deepfakes faster.
- The authors should consider possible harms that could arise when the technology is being used as intended and functioning correctly, harms that could arise when the technology is being used as intended but gives incorrect results, and harms following from (intentional or unintentional) misuse of the technology.
- If there are negative societal impacts, the authors could also discuss possible mitigation strategies (e.g., gated release of models, providing defenses in addition to attacks, mechanisms for monitoring misuse, mechanisms to monitor how a system learns from feedback over time, improving the efficiency and accessibility of ML).

#### 11. **Safeguards**

Question: Does the paper describe safeguards that have been put in place for responsible release of data or models that have a high risk for misuse (e.g., pretrained language models, image generators, or scraped datasets)?

Answer: [NA]

Justification: The models and data used in the research do not have any risk for misuse.

Guidelines:

- The answer NA means that the paper poses no such risks.
- Released models that have a high risk for misuse or dual-use should be released with necessary safeguards to allow for controlled use of the model, for example by requiring that users adhere to usage guidelines or restrictions to access the model or implementing safety filters.
- Datasets that have been scraped from the Internet could pose safety risks. The authors should describe how they avoided releasing unsafe images.
- We recognize that providing effective safeguards is challenging, and many papers do not require this, but we encourage authors to take this into account and make a best faith effort.

#### 12. **Licenses for existing assets**

Question: Are the creators or original owners of assets (e.g., code, data, models), used in the paper, properly credited and are the license and terms of use explicitly mentioned and properly respected?

Answer: [NA]

Justification: The third-party deep learning frameworks (JAX, Optax, Equinox) used in this work are appropriately cited. All models and datasets were developed and implemented independently by the authors.

Guidelines:

- The answer NA means that the paper does not use existing assets.
- The authors should cite the original paper that produced the code package or dataset.
- The authors should state which version of the asset is used and, if possible, include a URL.
- The name of the license (e.g., CC-BY 4.0) should be included for each asset.
- For scraped data from a particular source (e.g., website), the copyright and terms of service of that source should be provided.
- If assets are released, the license, copyright information, and terms of use in the package should be provided. For popular datasets, [paperswithcode.com/datasets](https://paperswithcode.com/datasets) has curated licenses for some datasets. Their licensing guide can help determine the license of a dataset.
- For existing datasets that are re-packaged, both the original license and the license of the derived asset (if it has changed) should be provided.
- If this information is not available online, the authors are encouraged to reach out to the asset's creators.

### 13. New assets

Question: Are new assets introduced in the paper well documented and is the documentation provided alongside the assets?

Answer: [NA]

Justification: The article does not release new assets.

Guidelines:

- The answer NA means that the paper does not release new assets.
- Researchers should communicate the details of the dataset/code/model as part of their submissions via structured templates. This includes details about training, license, limitations, etc.
- The paper should discuss whether and how consent was obtained from people whose asset is used.
- At submission time, remember to anonymize your assets (if applicable). You can either create an anonymized URL or include an anonymized zip file.

### 14. Crowdsourcing and research with human subjects

Question: For crowdsourcing experiments and research with human subjects, does the paper include the full text of instructions given to participants and screenshots, if applicable, as well as details about compensation (if any)?

Answer: [NA]

Justification: No human subjects were involved in our research.

Guidelines:

- The answer NA means that the paper does not involve crowdsourcing nor research with human subjects.
- Including this information in the supplemental material is fine, but if the main contribution of the paper involves human subjects, then as much detail as possible should be included in the main paper.
- According to the NeurIPS Code of Ethics, workers involved in data collection, curation, or other labor should be paid at least the minimum wage in the country of the data collector.

### 15. Institutional review board (IRB) approvals or equivalent for research with human subjects

Question: Does the paper describe potential risks incurred by study participants, whether such risks were disclosed to the subjects, and whether Institutional Review Board (IRB) approvals (or an equivalent approval/review based on the requirements of your country or institution) were obtained?

Answer: [NA]

Justification: No human subjects were involved in our research.

Guidelines:

- The answer NA means that the paper does not involve crowdsourcing nor research with human subjects.
- Depending on the country in which research is conducted, IRB approval (or equivalent) may be required for any human subjects research. If you obtained IRB approval, you should clearly state this in the paper.
- We recognize that the procedures for this may vary significantly between institutions and locations, and we expect authors to adhere to the NeurIPS Code of Ethics and the guidelines for their institution.
- For initial submissions, do not include any information that would break anonymity (if applicable), such as the institution conducting the review.

#### 16. **Declaration of LLM usage**

Question: Does the paper describe the usage of LLMs if it is an important, original, or non-standard component of the core methods in this research? Note that if the LLM is used only for writing, editing, or formatting purposes and does not impact the core methodology, scientific rigor, or originality of the research, declaration is not required.

Answer: [NA]

Justification: The core method development in this research does not involve LLMs as any important, original, or non-standard components.

Guidelines:

- The answer NA means that the core method development in this research does not involve LLMs as any important, original, or non-standard components.
- Please refer to our LLM policy (<https://neurips.cc/Conferences/2025/LLM>) for what should or should not be described.